J. Cosmet. Sci., 64, 355–370 (September/October 2013)

Determination of physicochemical properties of delipidized hair

ROGER L. McMULLEN, DONNA LAURA, SUSAN CHEN, DONALD KOELMEL, GUOJIN ZHANG, and TIMOTHY GILLECE, *Materials Science Department, Corporate R&D, Ashland Specialty Ingredients, Wayne, NJ 07470.*

Accepted for publication April 22, 2013.

Synopsis

Using various physicochemical methods of analysis, we examined human hair in its virgin and delipidized state. Free lipids were removed by a solvent extraction technique (covalently bound lipids were not removed) using a series of solvents with varying polarity. We analyzed the surface properties of hair by conducting mechanical combing and dynamic contact angle analysis. In addition, we used inverse gas chromatography surface energy analysis to explore the chemical composition of the hair surface based on interactions of various nonpolar and polar probes with biological molecules residing on the hair surface. Further, we investigated the importance that free lipids play in the internal structural properties of hair using dynamic scanning calorimetry and tensile strength measurements. The microstructure of the hair surface was probed by atomic force microscopy, whereas the lipid content of hair's morphological components was determined by infrared spectroscopic imaging. We also monitored the water management properties of virgin and delipidized hair by dynamic vapor sorption, which yielded unique water sorption isotherms for each hair type. Using all these techniques, differences were found in the chemical composition and physical behavior of virgin and delipidized hair. To better understand the influence of hair lipid composition on hair styling treatments, we conducted mechanical analyses of hair shaped into omega loops to determine the stiffness, elasticity, and flexibility of hair–polymer assemblies. Although there were no discernible differences between untreated virgin and delipidized hair, in terms of stiffness and elasticity, we found that treatment with hair styling agents produced different effects depending on the hair type used. Likewise, streaming potential measurements were carried out to monitor the binding capacity of rinse-off treatments on virgin and delipidized hair. Using this technique, we monitored the surface potential of hair and found significant differences in the binding behavior of cationic polymers and surfactants (polyquaternium-55 and quaternium-26) on both hair types.

INTRODUCTION

Lipids play an important role in the functional and structural properties of hair. They are often designated as surface or internal lipids, and can be of sebaceous origin, or they may carry out a structural role. The structural lipids can be covalently bound [e.g., 18-methyleicosanoic acid (18-MEA) on the surface] or free (e.g., free fatty acids, cholesterol, ceramides, etc.).

Address all correspondence to Roger McMullen at rmcmullen@ashland.com.

They carry out a structural role by providing hair with a cell membrane complex (CMC), present in both cuticle and cortical cells. In recent years, insight has been gained as to the structural details of the CMC for both cuticle and cortical cells as well as the interface between the cuticle and cortex (1). There are two parts of the cuticle CMC, which are normally classified as the upper and lower β layers. The upper β layer contains covalently-bound 18-MEA, which is believed to form a monolayer interspersed with other free fatty acids, which are presumably stabilized by van der Waals and electrostatic interactions. The upper β layer is located on the uppermost lamina of the cuticle cell and is exposed to the external environment. It is also present at the top of each underlying cuticle cell where it comes in contact with the lower β layer of an overlying cell. Located on the underside of the cuticle cell, the lower β layer consists of a monolayer containing free fatty acids and covalently attached fatty acids (but, no 18-MEA). The lower β layer of an overlying cell is separated from the upper β layer of an underlying cell by the delta layer, intercellular cement holding the two cells together, which is thought to be glycoprotein or globular protein (Fig. 1).

Unlike the upper and lower β layers in the cuticle, which contain a mixture of covalently and noncovalently attached lipids, the CMC of cortical cells consists of free fatty acids, cholesterol (or cholesterol sulfate), and ceramide (1). The outer edge of each cortical cell is surrounded by a bilayer structure, the cortical CMC, which is further enveloped by a delta layer that acts as the interface with another cortical cell. Thus, two bilayers from adjacent cortical cells are separated by a thin delta layer (Fig. 2). The interface between cuticle and cortical cells is a composite CMC composed on the cuticle side of a mixed monolayer of covalently and noncovalently attached fatty acids (lower β layer) and on the cortical side of a bilayer of free fatty acids, cholesterol, and ceramide. The cuticle monolayer and cortical bilayer are also separated by a delta layer.

In the last several decades, considerable attention in the research community has been given to structural lipids, especially covalently bound 18-MEA (2–4). Lipids of sebaceous origin were often deemed as less important, or even a nuisance, and thought to play little or no functional role in hair. In skin, sebum is an integral component that carries out a protective functional role. Sebaceous secretions provide a lipid-rich hydrophobic substance that protects the outermost surface of skin, thereby enhancing barrier function. They also transport antioxidants and antimicrobial peptides to the skin surface to protect

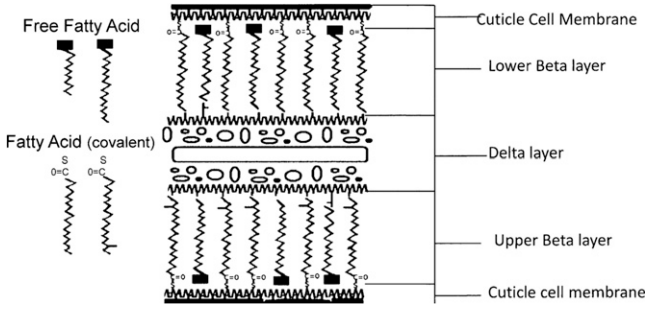

Figure 1. Schematic of the CMC (lower and upper β layers) of two overlying cuticle cells. The lower β layer corresponds to the overlying cell whereas the upper β layer corresponds to the underlying cell. Reprinted with permission from Society of Cosmetic Chemists. Copyright 2009. Originally appeared in Reference 1.

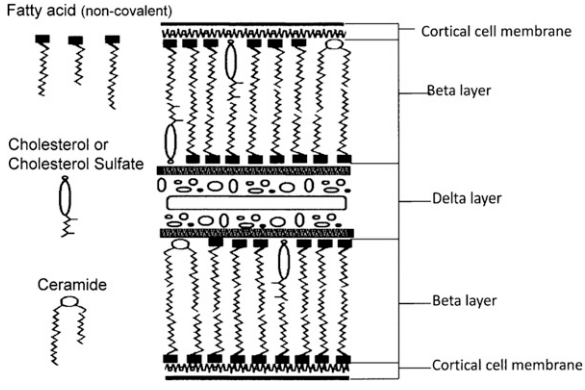

Figure 2. Schematic of the cortical CMC of two adjacent cortical cells separated by a delta layer. Reprinted with permission from Society of Cosmetic Chemists. Copyright 2009. Originally appeared in Reference 1.

it from environmental insult (e.g., UV radiation) and invasion by foreign pathogens. Sebaceous lipids consist of free fatty acids, triglycerides, free cholesterol, cholesterol and wax esters, paraffins, and squalene.

In this work, we investigated the physicochemical properties of delipidized hair using cutting-edge instrumental techniques to probe the surface and interior of the fiber structure. During our extraction procedure, we removed both sebaceous lipids and free structural lipids from the exterior and interior of the fiber. For this reason, it is difficult to discern differences in the structural/functional contributions of measured fiber properties by either sebum or free structural lipids. It should be noted though that we do not remove covalently attached lipids (e.g., 18-MEA) from hair. Therefore, any changes we observe in the physicochemical properties of delipidized hair by solvent extraction are due to free structural lipids or lipids of sebaceous origin.

MATERIALS AND METHODS

Studies were conducted on virgin and delipidized hair. We removed noncovalently attached lipids from hair using a Soxhlet extraction technique. Various instrumental techniques were used to examine differences between virgin and delipidized hair and to discover the importance of these lipids in the physicochemical behavior of hair. Details of each experimental technique are provided in the following sections.

DELIPIDIZATION OF HAIR

Using a Soxhlet extraction apparatus, free internal and surface lipids were removed from hair. This method is based on an established procedure in which hair is extracted with a series of solvents of increasing polarity (5). The apparatus consisted of a round bottom flask to which a Soxhlet extraction tube was mounted. Inside the Soxhlet extraction tube, a bundle of hair was placed in a cellulose thimble. A condenser was mounted on top of the Soxhlet extraction tube. The effect of solvent extraction on hair was investigated first by treatment with t-butanol and *n*-hexane for 4 h each, then with a mixture of chloroform/methanol

(70:30, v/v) for 6 h. In each procedure, 3 g of hair was treated with 250 ml of solvent in the Soxhlet extractor.

MECHANICAL COMBING MEASUREMENTS

Combing analysis was achieved using a miniature tensile tester (Model 170), manufactured by Dia-Stron, Ltd., Hampshire, United Kingdom. The combing measurements were carried out on wet and dry hair with the following instrumental parameters: range, 2000 G; gauge, 2 G; size, 50 mm; phase 1 (extension), 350%; phase 2, 0%; phase 3, 0%; and phase 4, 0%. In all experiments, hair tresses were combed several times to remove entanglements before performing combing measurements.

DYNAMIC CONTACT ANALYSIS

A Thermo Cahn Dynamic Contact Angle Analyzer, DCA-322 (Thermo Fisher Scientific, Waltham, MA), was used to determine contact angle. A single dry hair fiber, cut to approximately 1 cm, was immersed in deionized water approximately 2–4 mm and the advancing contact angle was measured (inserted tip end first). Fibers were obtained from the middle of a hair tress assembly ensuring that a straight section of fiber was sampled. The required hair diameters were measured using a laser micrometer (Mitutoyo, model LSM-5000) purchased from Dia-Stron, Ltd. Twenty fibers each for virgin and delipidized hair were measured.

ATOMIC FORCE MICROSCOPY

Atomic force microscopy (AFM) studies were conducted using a Digital Instruments Nanoprobe III Multimode SPM manufactured by Veeco Instruments (Santa Barbara, CA). Two modes of analysis, AFM and lateral force microscopy (LFM), were carried out in the contact mode. An AFM/LFM probe head was used in conjunction with a 100 μm piezoelectric scanner. The instrument used is a "beam bounce" type in which a diode laser beam is focused on to the back (top) of the cantilever. Commercial AFM probes (silicon tip on nitride lever, model SNL-10) were purchased from Veeco. Three-dimensional topography, error signal, and lateral force images were generated and analyzed with the instrument software (NanoScope Software, Veeco, Santa Barbara, CA).

FTIR SPECTROSCOPIC IMAGING

A 1-cm-long hair bundle was cut from the middle of Asian hair tresses and mounted on the top of a sample holder by embedding in ice. The hair bundle was then microtomed at -30°C into 5 μm thick cross sections with a Leica CM 1850 cryostat (Leica Microsystems, Inc., Bannockburn, IL). Hair cross sections were collected onto CaF_2 windows for IR imaging. This preparation technique avoids any possibility of contamination with embedding or fixing medium. Hair cross sections were imaged with a Perkin Elmer Spotlight system that couples an FTIR spectrometer with an optical microscope. The system consists of a linear

array of mercury-cadmium-telluride detector and an automated high precision XY sample stage. Images were acquired with 6.25 μm step size, 8 scans for each spectrum and 8 cm^{-1} spectral resolution. IR spectra were analyzed using ISys 3.1 software (6).

DIFFERENTIAL SCANNING CALORIMETRY

A Q2000 differential scanning calorimeter (TA Instruments, New Castle, DE) was used with pressure resistant, high-volume stainless steel pans. Samples consisted of 8 to 12 mg of cut (2–5 mm) hair fibers, along with roughly 55 (±1.5) mg of deionized water. Each pan was sealed and allowed to sit for at least 6 h at room temperature to insure equilibrium water content and distribution within the hair fibers. Heating at a rate of 2°C was performed from 22 to 190°C in standard mode. Three repetitions per lot were conducted. TA Universal Analysis 2000 for Windows software, version 4.7A, was used to determine the denaturation temperature (T_d) and the enthalpy of denaturation (ΔH). Peak integrations were performed using the sigmoidal horizontal method, with the left marker staked at 110°C and the right positioned in the middle of the post-transition flat baseline section (typically just below 150°C).

TENSILE STRENGTH

An Instron (model 3345) universal testing system for compression and tension, manufactured by Instron (Norwood, MA), was used for tensile strength measurements. The instrument was equipped with a 100 N capacity force transducer (model 2519-103) and pneumatic grips (250 N capacity) with rubber-coated jaws capable of holding single hair fibers. Each fiber was mounted with metal and the samples were extended at a rate of 25 mm/min with data acquisition set at 100 Hz. Before tensile strength measurements, fiber diameters were determined with a laser micrometer (Mitutoyo, model LSM-5000) purchased from Dia-Stron, Ltd.

DYNAMIC VAPOR SORPTION ANALYSIS

A DVS Advantage-1 gravimetric vapor sorption analyzer from Surface Measurement Systems (Alperton, Middlesex, United Kingdom) was used. Hair samples consisted of approximately 25 fibers tied into a small loop weighing approximately 5 mg. The average diameter of the fibers of each sample was determined using a Mitutoyo laser micrometer (Dia-Stron, Ltd.). Samples were subjected to 0–90% RH at 25°C in steps of 10% RH followed by 90–0% RH in steps of 10% RH. Each sorption/desorption step was 8 h in duration. Data were analyzed using DVS Standard Analysis Suite V6.1.1, DVS Advanced Analysis Suite V6.1.1, and Isotherm Analysis Suite V2.1.1.

MECHANICAL ANALYSIS OF HAIR-SHAPED OMEGA LOOPS

The instrumentation and experimental procedures were similar to those used in previous work (7). In brief, omega loop hair tresses were constructed by gluing both ends of the hair

(approximately 0.3 g of 3.5-in. long hair) to square Plexiglas plates using Duco cement, leaving 1.5 in. of fibers between the tabs. The hair was wetted, then shaped into an omega loop using a Teflon rod, and allowed to dry at 50% RH for 12 h. Mechanical measurements were carried out with a Texture Analyzer (Stable Micro Systems, Godalming, United Kingdom). We first examine untreated hair, then we reinsert a Teflon rod in the omega loop so that treatment with styling resins may be administered. Polymer-treated omega loops are allowed to dry for 12 h at 50% RH followed by measurements.

STREAMING POTENTIAL ANALYSIS

In this study, we used streaming potential instrumentation, referred to as a dynamic electrokinetic and permeability analyzer, manufactured by Better Cosmetics, LLC (Bethel, CT) (8). This custom-built device allows for the collection of electrokinetic parameters (streaming potential and conductivity) as well as permeability of fiber plugs. The dynamic electrokinetic and permeability analyzer consists of a streaming potential cell, valve assembly controlling the flow of liquids, conductivity meter, pH and temperature meter, pressure controller, test and treatment solution reservoirs, and electronic balance flow meter.

INVERSE GAS CHROMATOGRAPHY SURFACE ENERGY ANALYSIS

All analyses were carried out using an inverse gas chromatography surface energy analyzer and the data were analyzed using both standard and advanced SEA Analysis Software. For all experiments, between 1.5 and 2.0 g of hair samples (entire strands) were packed into an individual silanized glass column (300 mm long by 4 mm inner diameter). The samples were run at a series of surface coverages with both alkanes (undecane, decane, nonane, octane and heptanes; only four alkanes were used for calculations) and polar probe molecules (ethanol, acetone, ethyl acetate, dichloromethane, and acetonitrile) to determine the dispersive surface energy as well as the acid–base free energy of desorption. In this study, each column was preconditioned for 1 h at 25°C and 30% RH with helium carrier gas to normalize all samples at a humidity representative of ambient conditions. At no time were the samples exposed to dry helium conditions, as not to induce irreversible changes to the hair fibers. All experiments were carried out at 25°C and 30% RH with a 10 sccm total flow rate of helium, and using methane for dead volume corrections.

MATERIALS

The majority of the experiments were performed on Asian hair purchased from International Hair Importers and Products, Inc., Glendale, NY. Hair tresses were prepared by gluing 2 g of fibers to a 1.5-in × 1.5-in Plexiglas tab with Duco Cement. The resulting dimensions of the hair tresses were 6.4 inch in length and 1.25 inch in width. Hair tresses were precleaned with a 3% ammonium lauryl sulfate solution and rinsed thoroughly before use in the experiments. Rinse-off treatments were administered with polyquaternium-55 and quaternium-26, which are commercial products by Ashland, Inc. (Covington, KY)

sold under the trade names Styleze W and Ceraphyl 65, respectively. Styling treatments consisted of various molecular weights of PVP manufactured by Ashland, Inc. under the tradenames of PVP K-15 (M_w = 8,000), PVP K-30 (M_w = 60,000), PVP K-60 (M_w = 400,000), PVP K-90 (M_w = 1,300,000), and PVP K-120 (M_w = 3,000,000).

RESULTS AND DISCUSSION

We investigated the physicochemical properties of hair contributed by its free lipid components. By subjecting hair to a series of solvent extractions, we were able to effectively remove noncovalently bound lipids and, thus, make comparisons with virgin hair containing its normal lipidic components. Many of the techniques used in this study yielded results demonstrating that noncovalently bound lipids influence various properties of hair.

INVESTIGATION OF HAIR BIOPHYSICS/BIOCHEMISTRY

The chemical compositional changes including lipid loss, protein conformation, and water binding capacity were monitored by FTIR spectroscopic imaging (6). In our examination of cross sections of hair, we generate images that qualitatively show the distribution for selective wavelength regions of the infrared spectrum that correspond to a biophysical feature of hair morphology. For example, by monitoring the lipid band at 2850 cm^{-1} (methylene asymmetric stretching), we can generate an image of the cross section of hair that shows the distribution of lipid in the cuticle, cortex, and medulla. In virgin hair, we generally see most of the lipids are concentrated in the medulla. When we extract hair with *n*-hexane we find that surface lipids are removed, but lipids within the internal structure of hair remain. It is not until hair is rigorously extracted with chloroform/methanol (70:30) that all of the lipids are removed. FTIR spectroscopic images of the lipid distribution in hair cross sections are shown in Fig. 3. As depicted by the scale, dark colors in the image (blue) indicate lower concentrations of lipid while brighter colors (yellow/orange/brown) are due to higher concentrations of lipid. In virgin hair, especially of Asian origin, we note that the greatest concentration of lipids tends to be in the medulla region of hair. This was discussed in greater detail in a previous publication (6). Examining Fig. 3, we can clearly see that delipidized hair contains much lower concentrations of lipid across the entire fiber cross section than virgin hair.

HAIR SURFACE ANALYSIS

To probe the surface properties of hair we used dynamic contact angle analysis, mechanical combing measurements, and AFM. Changes in the molecular properties of materials lead to changes in their macroscale properties. For example, the wetting properties of a surface can change due to chemical modification. We measured the DCA using single fiber (Wilhelmy) methodology. In this technique, a hair fiber is anchored to a microbalance then immersed in H_2O. On the basis of the wettability of the fiber in water, contact angle determinations can be made using the following equation:

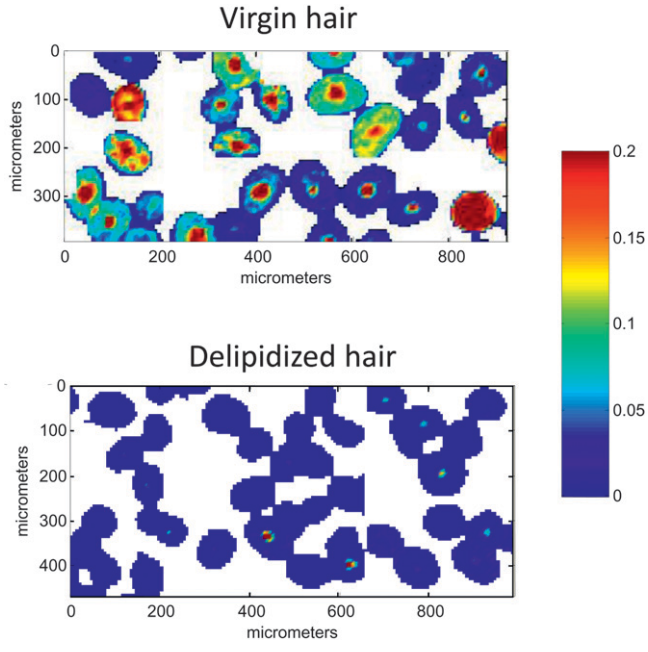

Figure 3. FTIR spectroscopic imaging of hair cross sections obtained by monitoring the lipid peak (2850 cm^{-1}).

$$F \bullet g = \gamma \bullet PR \bullet \cos\theta \quad (1)$$

In this case, F is the interaction force between hair fiber and water (called wetting force), g is the gravitational constant, γ is the surface tension of water, PR is the wetted perimeter of solid, and θ is the contact angle between hair and water. For hair fibers, PR equals πD (D is the hair fiber diameter). On the basis of our studies of the two hair types, we observed a decrease in DCA from $95.72 \pm 6.21°$ for virgin hair to $79.60 \pm 7.12°$ for delipidized hair. For comparison with previously obtained measurements in the literature, values of $103 \pm 4°$ and $98 \pm 2°$ were obtained for dry and soaked virgin caucasian hair, respectively (9). Typically, chemical damage to the hair surface (e.g., from bleaching, permanent waving, etc.) results in contact angle measurements ranging from 70 to 80°.

Combing measurements show increases in both dry and wet combing forces of delipidized hair. Such a result is not surprising because adding oils to hair facilitates combing. Thus, the contrary should be true when lipids are removed from hair. Table I contains wet combing data that were obtained by integrating the entire combing curve. Clearly, a distinction may be made between virgin (0.061 g cm) and delipidized (0.325 g cm) hair, with the latter being more than five times more difficult to comb. The increase in combing of delipidized wet fibers reflects the greater influence of capillary forces in this hair type, presumably due to its more hydrophilic surface.

Likewise, we found appreciable differences between both hair types when examining dry combing curves. Typically, dry combing curves begin with very low combing forces (root section and middle of the tress) followed by a large peak corresponding to the bottom of the tress where the tips of the fibers become entangled. To differentiate various effects in

Table I
Wet Combing Work Values for Virgin and Delipidized Hair

Hair type	Combing work (g cm)
Virgin	0.061 ± 0.0071
Delipidized	0.325 ± 0.0450

the dry combing analysis we examined several regions of the dry combing curves (Table II). In our initial analysis, we compared the maximum peak intensity corresponding to the entanglement peak in which case dry combing of delipidized hair resulted in an increase over five times greater than virgin hair. The total combing work is also reported in Table II and represents the integrated values for the entire dry combing curves including the entanglement peak region. We also examined the integrated values of dry combing curves up to, but not including, the entanglement peak. In addition, we also integrated only the entanglement peak region. Overall, all portions of the drying combing curve are more difficult to comb in the case of delipidized hair. The smallest difference between the two hair types is in the region up to, but not including, the entanglement peak. Typically, this is the most difficult region of the combing curve to differentiate. Please bear in mind that the data reported are statistically significant and represent averages of five hair tresses combed five times for both wet and dry combing analysis.

AFM investigations were carried out in contact mode while monitoring topography and lateral forces. A striking feature we found in delipidized hair was the presence of many micropores. Figure 4 provides a representative example on solvent-extracted hair in which a considerable population of micropores can be seen. The average diameter of the pores was determined to be 150 ± 25 nm with their depth estimated to be 8.0 ± 2.5 nm. The pore depth may be greater than the measured value because of limitations of the probe to reach the bottom of the pore. We examined four hair fibers from each population and obtained 25 images at randomly selected positions along the hair shaft. In virgin hair, we found micropores in only 21% of the sites examined, whereas they were present 70% of the time in delipidized hair. Interestingly, we also observed micropores in 42% of the cases for hair that underwent a standard bleaching procedure. It is likely that the pores are a part of the natural anatomic structure of the hair fiber and only become revealed when surface lipids are removed (10).

HEALTH STATE OF INTERNAL HAIR STRUCTURE

Information about the importance that free lipids play in the structural properties of hair was investigated using differential scanning calorimetry (DSC) and tensile strength

Table II
Dry Combing Work Values for Virgin and Delipidized Hair

Hair type	Peak max (g)	Combing work (g cm)—total	Combing work (g cm)—up to but not including peak	Combing work (g cm)—peak
Virgin	106.24 ± 11.52	0.028 ± 0.0027	0.017 ± 0.0018	0.011 ± 0.0010
Delipidized	559.48 ± 95.02	0.065 ± 0.0066	0.0276 ± 0.0025	0.038 ± 0.0050

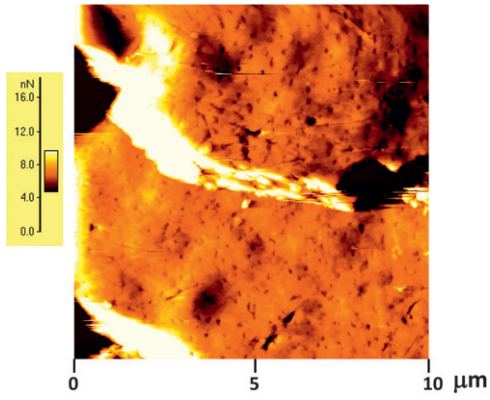

Figure 4. AFM error signal image (10 µm) of solvent-extracted hair revealing micropores on the hair surface. Originally appeared in Reference 9.

measurements with an Instron. DSC results did not show any difference in the hair's crystalline phase behavior whether, or not, lipids were present. The ΔH and T_d values were similar for both virgin and delipidized hair: $\Delta H = 22.99 \pm 0.49$ J/g and $T_d = 142.86 \pm 0.19°$ C for virgin hair and $\Delta H = 22.33 \pm 0.83$ J/g and $T_d = 142.46 \pm 0.20°$ C for delipidized hair. Tensile strength measurements were also carried out resulting in stress–strain curves, which were analyzed for key parameters related to the mechanical tensile properties of hair. We specifically monitored the Young's modulus (slope in the Hookean region) and the stress at break (maximum force required to break the fiber). Studies were carried out on 100 fibers from each population set in a controlled environment of 25° C and 45% RH. Histograms were generated for each measured value for both hair types. The region where the maximum distribution on the histogram occurred is reported as the final value for both Young's modulus and stress at break. Both virgin and delipidized hair yielded Young's modulus values between 5×10^{10} and 10×10^{10} dynes/cm^2. Likewise, we found the stress at break was similar for both hair types with maximum distributions at 2×10^8 to 2.5×10^8 dynes/cm^2. Although the maximum distributions in the histogram plots were the same for virgin and delipidized hair for both measured parameters, we did find it interesting that the overall distributions were distinct. Delipidized hair had much broader distributions than virgin hair, which usually contained a very sharp peak at its maximum distribution value. In conclusion, results of the mechanical measurements and DSC of hair provide evidence that the internal structure of hair is not damaged because of lipid removal.

EFFECTS OF HAIR TREATMENTS ON DELIPIDIZED HAIR

To understand the impact of cosmetic products on delipidized hair, we treated hair with various ingredients, such as conditioning surfactants, cationic polymers, and nonionic/anionic polymeric resins. Our findings suggest that these treatments are greatly influenced by the lipid content of hair. Streaming potential analysis shows that cationic species (e.g., surfactant or polymer) interact differently with delipidized hair than with its virgin counterpart. Mechanical measurements (stress–strain curves) were also conducted

on hair shaped into omega loops. Although there were no discernible differences between untreated virgin and untreated delipidized hair, in terms of stiffness and elasticity, we found that treatment with hair styling agents produced different effects depending on the hair type used.

Using streaming potential measurements, we compared the affinity of polyquaternium-55 and quaternium-26 to virgin and delipidized hair and found that their binding capacity depends on the lipid composition of hair. Figures 5 and 6 contain plots of streaming potential as a function of treatment time for virgin and delipidized hair treated with a cationic surfactant (quaternium-26) and polymer (polyquaternium-55). As shown in Fig. 6, initial readings (only in KCl solution) for the streaming potential plot were normalized. In fact, under normal circumstances untreated hair has a negative charge resulting in negative streaming potential values. In any event, our decision to normalize the data was based on our desire to monitor any differences between the two hair types. Figure 6 shows the changes experienced by a plug of hair during a treatment cycle with quaternium-26. After treatment (2000 s), the streaming potential spikes followed by a decay corresponding to the rinse cycle (with KCl solution). After extended rinsing, a steady state is eventually reached where the streaming potential values level off. The difference between surfactant- and polymer-treated hair is striking. As illustrated in Fig. 6, the degree of decay in the streaming potential for hair treated with a cationic polymer is much less than is the case with a cationic surfactant. Such a phenomenon can be explained by the greater affinity of cationic polymers to hair (multiple-binding sites), which cannot be easily removed, especially with water rinsing. It is interesting to note that the cationic surfactant and polymer have less affinity for delipidized hair. It is likely that binding of these compounds to the hair surface greatly relies on van der Waals stabilization, which would be facilitated by the presence of lipids. Hence, removal of lipids renders a surface free of other molecules which the cationic polymer and surfactant can associate with.

Various mechanical properties of hair fiber assemblies were measured using previously developed methodology in which hair is shaped into an omega loop and examined in its

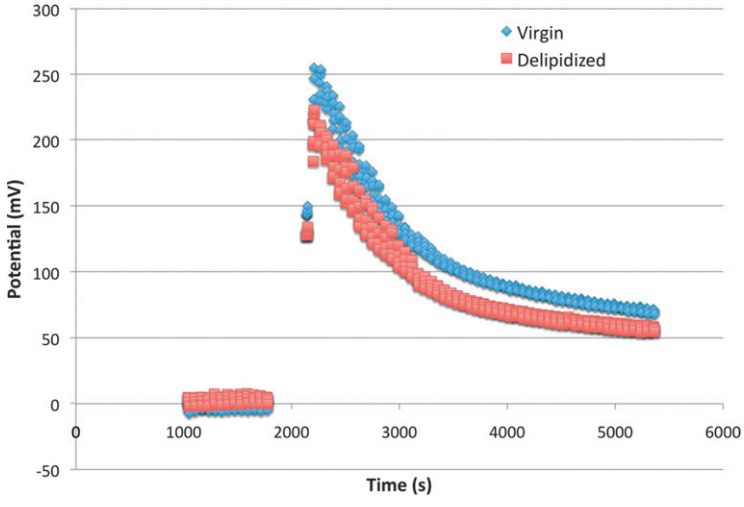

Figure 5. Streaming potential plot of virgin and delipidized hair treated with cationic surfactant (Quaternium-26).

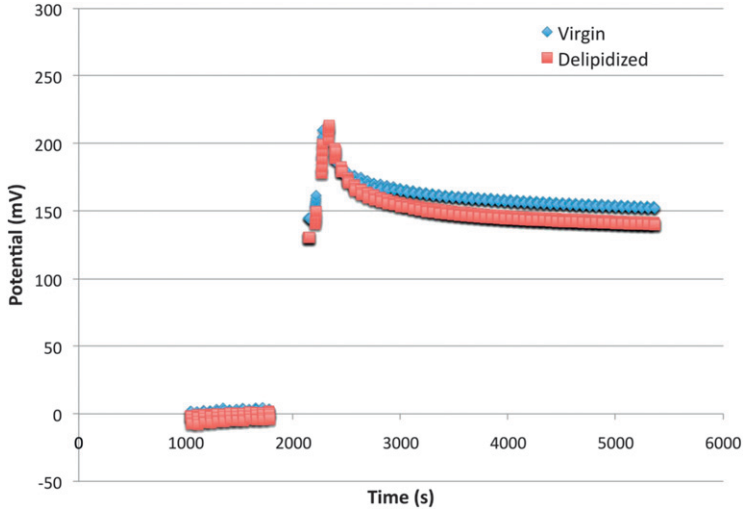

Figure 6. Streaming potential plot of virgin and delipidized hair treated with a cationic polymer (Polyquaternium-55).

untreated and treated states (7). Several parameters are monitored and include stiffness, elasticity, flexibility, and plasticity. Typically, this technique can be used to discern structure-function properties of materials. We also find that many of the measured properties are dependent on molecular weight. For example, high molecular weight species normally yield higher stiffness ratios and flexibility as opposed to their more brittle lower molecular weight counterparts. Figure 7 contains a plot of stiffness ratio for various grades of PVP with the following M_w values: PVP K-15 (M_w = 8,000), PVP K-30 (M_w = 60,000), PVP K-60 (M_w = 400,000), PVP K-90 (M_w = 1,300,000), and PVP K-120 (M_w = 3,000,000). As expected, stiffness of the omega loop polymer–fiber assembly increases with increasing molecular weight of the polymer. When comparing virgin and delipidized hair, we found that there was no difference in any of the measured parameters in the untreated state. However, treatment with the ensemble of PVP samples clearly illustrated a directional trend in the stiffness ratio measurements. When a polymeric resin (in this case, PVP) was applied to delipidized hair, the polymer–hair fiber assembly was stronger (higher stiffness) than virgin hair treated by the same regimen—an effect most likely determined by surface wetting characteristics of the chosen hair type, which would be governed by its lipid composition.

WATER MANAGEMENT PROPERTIES OF HAIR

We generated adsorption/desorption isotherms using DVS analysis to investigate if the water management properties of hair are greatly influenced by the presence, or absence, of lipids. This gravimetric technique monitors the solvent uptake by a material, in this case hair and water. DVS water sorption isotherms were generated by exposing hair to stepwise changes in RH—sorption for increasing humidity and desorption for decreasing humidity—starting from 0% to 90% RH and then from 90% to 0% RH. Overall, we found much greater uptake (sorption) in delipidized hair as compared to the virgin hair sample (Fig. 8). Examination of the hysteresis between sorption and desorption curves

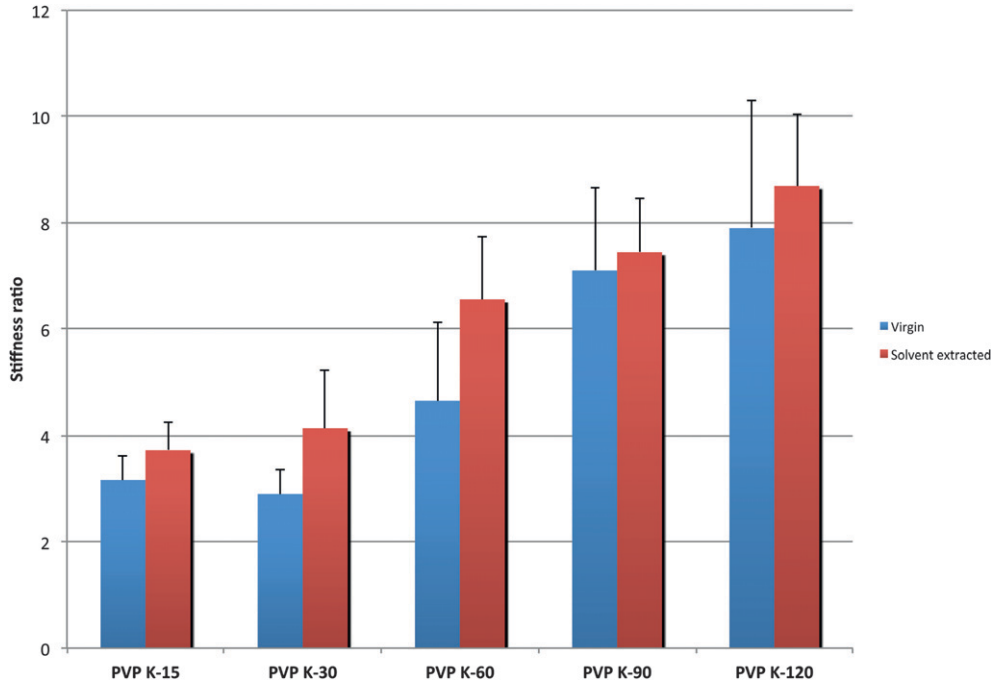

Figure 7. Stiffness ratio values for virgin and delipidized hair treated with various molecular weight samples of PVP.

reveals greater hysteresis values in the case of delipidized hair indicating more resistance to release water. One should bear in mind that generation of DVS isotherms of hair fibers is a kinetically governed process. For example, a study by Wortmann *et al.* (11) revealed no difference in the water sorption or desorption properties when comparing virgin, damaged, and hair treated with a cationic surfactant. More than likely, their experiments were carried for extended periods of time allowing full equilibration to be reached. Such experiments, when done properly, can take several weeks to complete for one sample. Often, shorter equilibration periods are used so that data may be obtained in a reasonable amount of time. One should also consider what types of equilibration time frames are reasonable in terms of the daily climatic experiences of a hair fiber.

SURFACE ENERGY ANALYSIS

We used inverse gas chromatography surface energy analysis (iGC SEA) to probe the surface energy profile of hair, which contains a dispersive $\left(\gamma_s^d\right)$ and acid–base component $\left(\gamma_s^{AB}\right)$ that contribute to the total surface energy $\left(\gamma_s^T\right)$:

$$\gamma_s^T = \gamma_s^d + \gamma_s^{AB} \qquad (1)$$

The dispersive surface energy accounts for the London dispersion forces, van der Waals forces, and Liftschitz interactions, whereas the acid–base component takes into consideration acid–base and polar interactions. The dispersive surface energy analysis was performed by measuring the net retention volume V_N (measured retention volume minus

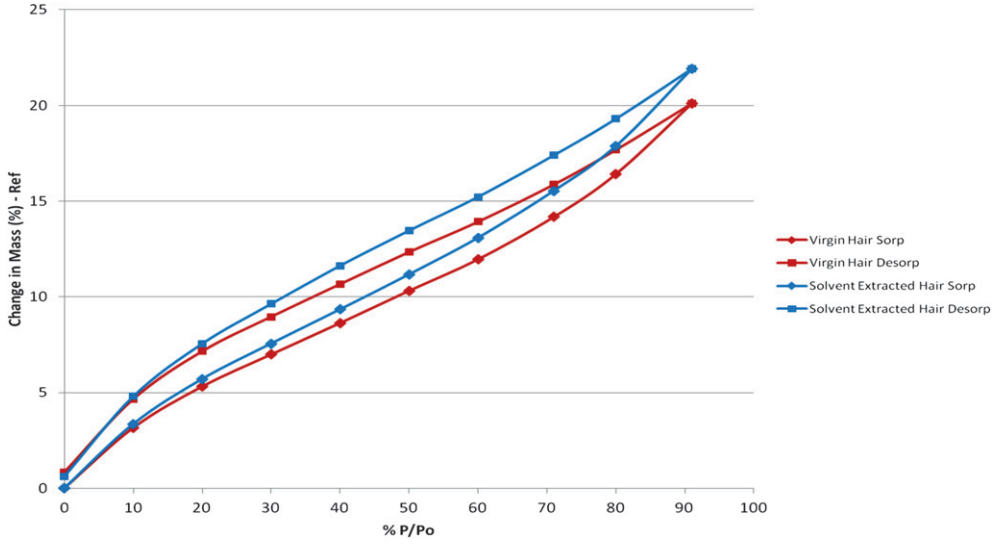

Figure 8. Sorption and desorption isotherms for virgin and delipidized hair.

dead volume) for a series of alkane elutants (in this case, heptane, octane, nonane, and decane). For the analysis, the method of Dorris and Gray was applied. In this method, a plot of $RT\ln(V_N)$ vs the carbon number (of the alkanes) should produce a linear regression. The dispersive component of the solid sample can then be determined from the slope of the regression. Overall, we observe that the dispersive surface energy is greater for virgin (~55 mJ/m^2) than delipidized (~48 mJ/m^2) hair at low surface coverage. The dispersive surface energy distribution is also more heterogenous for virgin hair. Such as result is consistent with expectations as the sample containing less lipid should interact less with the hydrocarbon probe samples in terms of van der Waals and other nonpolar interactions. In addition, because there should be a greater variety of lipid species on the surface of virgin hair, we expect a larger dispersive energy distribution.

The acid–base component of the total surface energy (also called specific surface energy) is obtained via iGC SEA by first measuring the specific free energies of desorption for different polar probe molecules, ΔG_{SP}. These values were determined by measuring the retention volume of polar probe molecules (ethanol, acetone, ethyl acetate, and chloroform) on the hair samples. In the polarization approach, the ΔG_{SP} values are determined from a plot of $RT\ln(V_N)$ vs the molar deformation polarization of the probes, P_D. Points representing a polar probe are located above the alkane straight line in the $RT\ln(V_N)$ vs P_D plot. The distance to the straight line is equal to the specific component of the free energy of desorption, ΔG_{SP}. From the ΔG values, one can calculate acid–base numbers which are related to the specific surface energy. Although the acid–base surface energy values are similar for both hair types—ranging from ~5.75 to 6.25 mJ/m^2—the distribution is broader for the delipidized sample. This could indicate that once the layer of lipids is removed from hair surface, the probes experience a greater variety of polar interactions due to the underlying exposed protein side chains.

In addition, Guttman (k_a and k_b) values were calculated from the specific energy data. k_a and k_b, respectively, provide information about the electron-donating and electron-accepting

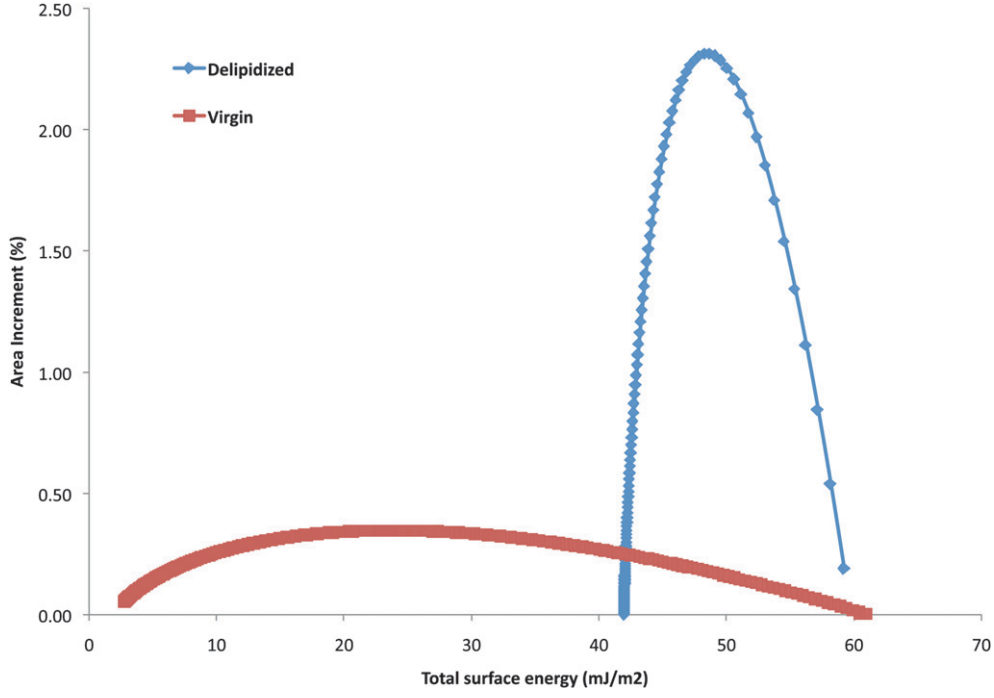

Figure 9. Total surface energy distributions of virgin and delipidized hair obtained by iGC SEA. The units are percentage of covered surface (where the total surface covered is determined by BET) vs extrapolated total surface energy (mJ/m^2).

characteristics of a surface. Delipidized hair yields lower k_b and higher k_a values than virgin hair indicating that its surface is more acidic (less basic) due to the removal of lipids. It is possible that once free lipids are removed from the surface, pendant groups on amino acids of upper layer cuticular structural proteins are exposed rendering the hair surface more acidic.

Extrapolated total surface energy distributions obtained from iGC SEA provide a representative illustration of changes in the surface chemistry of hair that occur as a result of delipidization. Figure 9 contains profiles for both hair types tested. The data were fitted to an empirical function and converted into a normalized distribution to display the surface energy results in a more illustrative manner. This total surface energy distribution estimates the percentage of both dispersive and acid–base sites at a particular surface energy. Interestingly, virgin hair has a much broader distribution, indicative of its very heterogenous surface characteristics. In contrast, delipidized hair has a very sharp total surface energy distribution as a result of its more homogenous surface.

CONCLUDING REMARKS

In the last several decades, we have witnessed studies searching for the importance of covalently attached 18-MEA in determining the surface properties of hair (2–4). Herein, we provide evidence that supports an indispensable role of noncovalently bound lipids in

the surface properties of human hair. Moreover, we show the importance of noncovalently bound lipids not only in governing the properties of hair, but also how they influence treatment with hair care products. In closing, the delipidization of hair represents a situation many consumers find themselves in after undergoing a harsh cosmetic procedure, or due to natural or environmental aging of the mature hair shaft.

ACKOWLEDGMENTS

We express our sincere gratitude to Dr. Dan Burnett from Surface Measurements Systems, Ltd., for his contribution of the section involving iGC SEA.

REFERENCES

(1) C. R. Robbins, The cell membrane complex: Three related but different cellular cohesion components of mammalian hair fibers, *J. Cosmet. Sci.,* **60,** 437–465 (2009).
(2) L. N. Jones and D. E. Rivett, 18-Methyleicosanoic acid in the structure and formation of mammalian hair fibres, *Micron,* **28,** 469–485 (1997).
(3) L. Coderch, S. Méndez, C. Barba, R. Pons, M. Martí, and J. L. Parra, Lamellar rearrangement of internal lipids from human hair, *Chem. Phys. Lipids,* **155,** 1–6 (2008).
(4) J. Smith and J. Swift, Maple syrup urine disease hair reveals the importance of 18-methyleicosanoic acid in cuticular delamination, *Micron,* **36,** 261–266 (2005).
(5) P. W. Wertz and D. T. Downing, Integral lipids of mammalian hair, *Comp. Biochem. Physiol.,* **92B,** 759–761 (1989).
(6) G. Zhang, L. Senak, and D. J. Moore, Measuring changes in chemistry, composition, and molecular structure within hair fibers by infrared and Raman spectroscopic imaging, *J. Biomed. Opt.,* **16**(5), 056009 (2011).
(7) J. Jachowicz and R. McMullen, Mechanical analysis of elasticity and flexibility of virgin and polymer-treated hair fiber assemblies, *J. Cosmet. Sci.,* **53,** 345–361 (2002).
(8) J. Jachowicz, Fingerprinting of cosmetic formulations by dynamic electrokinetic and permeability analysis, II. Hair conditioners, *J. Soc. Cosmet. Chem.,* **46,** 100–116 (1995).
(9) R. A. Lodge and B. Bhushan, Wetting properties of human hair by means of dynamic contact angle measurement, *J. Appl. Poly. Sci.,* **102,** 5255–5265 (2006).
(10) R. McMullen and S. P. Kelty, Investigation of human hair fibers using lateral force microscopy, *Scanning,* **23,** 337–345 (2001).
(11) F.-J. Wortmann, A. Hullmann, and C. Popescu, Water management of human hair, *IFSCC Mag*., **10**(4), 317–320 (2007).